Optica Applicata, Vol. XVIII, No. 1, 1988

Numerical investigations of the imaging by curved holographic lens*

JERZY NOWAK, MAREK ZAJĄC

Institute of Physics, Technical University of Wrocław, Wybrzeże Wyspiańskiego 27, 50–370 Wrocław, Poland.

The imaging by a holographic lens was investigated, and the results of the imaging quality evaluation are presented in the paper. Two cases, coherent and incoherent illumination, were taken into account. It was assumed that the holo-lens was recorded on a flat or spherical surface. The influence of the input pupil location on the quality of imaging was also analysed. For some typical parameters of the lens recording and imaging geometries the chosen characteristics of the image were calculated; namely, light intensity distribution in the aberration spot, two-point resolution limit, images of Ronchi ruling for several spatial frequencies in coherent illumination, and mutual transfer function for incoherent illumination.

1. Introduction

Evaluation of imaging quality is one of the problems appearing frequently in optics. In classical optics, this quality may be assumed via examination of the coefficients describing III-order aberrations as well as transfer function or wave aberration. If coherent light is used for imaging those image quality measures are not sufficient. Examination of the images of some typical "test object" such as single point or bar test may be useful in such situation.

Apart from traditional glass lenses the holographic lenses find more and more applications. Investigation of their imaging quality seems to be an interesting task. It is also useful to search for possibilities of the imaging quality improvement for holographic lenses.

2. Theoretical background and assumptions

The holographic lens (holo-lens) is in fact a hologram of two spherical waves originating from the point sources P_1 and R located in the same line perpendicular to the hologram plane (Fig. 1). This line constitutes the holo-lens axis. A spherical wave originating from any other point source C and falling on the holo-lens is transformed by it into two waves which form two images: primary P'_3 and

* This paper has been sponsored by the Polish Ministry of Science and Higher Education, Project CPBP 01.06; and was presented at the VIII Czechoslovak–Polish Optical Conference in Palkovice, September 1986.

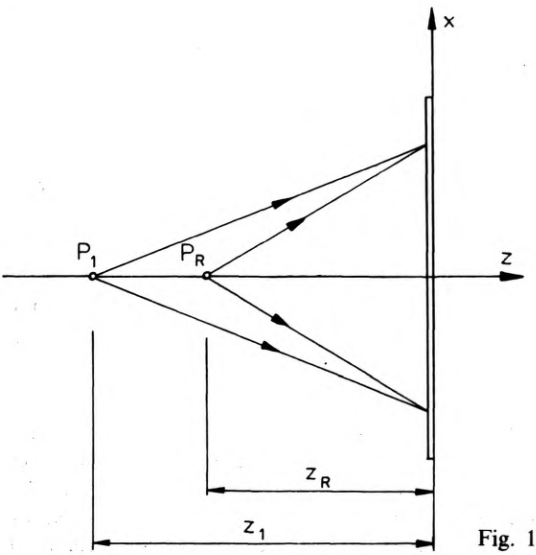

Fig. 1. Holo-lens recording geometry

secondary P_3'' (Fig. 2). Location of those images depends on the coordinates of the points P_1 and R as well as on the holo-lens scaling factor m and the ratio μ of the light wavelength used during imaging to that used during the holo-lens recording. The appropriate formula is a particular case of the respective expression derived for holographic imaging (e.g., [1], [2]) in which $x_1 = y_1 = x_R = y_R = 0$. In the Meier's expansion the Gauss image coordinates can be calculated as:

$$\begin{aligned} \frac{1}{z_3} &= \frac{1}{z_C} + \frac{1}{f}, \\ \frac{x_3}{z_3} &= \frac{x_C}{z_C}, \\ \frac{y_3}{z_3} &= \frac{y_C}{z_C} \end{aligned} \tag{1}$$

where $f = \pm \frac{m^2}{\mu}(1/z_1 - 1/z_R)^{-1}$ is a holo-lens focal distance.

It is evident that the completely aberration-free image can be obtained with a holo-lens; namely, if the object point C coincides with the point R during the holo-lens recording and $\mu = m = 1$, then one of the images (P_3') is free from any aberrations. However, such a geometry indicates that the object must lie on axis. The off-axis point object are always imaged imperfectly.

For evaluation of the aberrations connected with non-zero object field angle it is possible to use the well-known formulae derived in holography. For the holo-lens ($x_1 = y_1 = x_R = y_R = 0$) the coefficients describing the third-order aberrations in Meier's expansions are (for simplicity, only one-dimensional case will be discussed here):

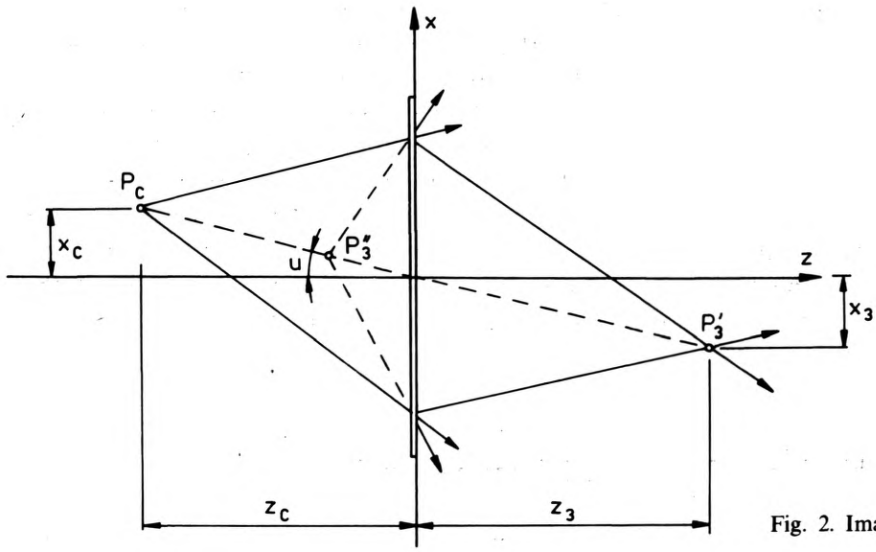

Fig. 2. Imaging geometry

Spherical aberration

$$S = \frac{1}{z_C^3} - \frac{1}{z_3^3} \pm \mu \left(\frac{1}{z_1^3} - \frac{1}{z_R^3} \right).$$

Coma

$$C = \frac{x_C}{z_C^3} - \frac{x_3}{z_3^3}.$$

Astigmatism

$$A = \frac{x_C^2}{z_C^3} - \frac{x_3^2}{z_3^3}.$$

Field curvature

$$F = A.$$

Distortion

$$D = \frac{x_C^3}{z_C^3} - \frac{x_3^3}{z_3^3}. \tag{2}$$

Coordinates of the Gauss image $P'_3(x_3, y_3, z_3)$ are related to those of the object point $C(x_C, y_C, z_C)$ by the formula (1) in which the holo-lens length f depends on the lens parameters z_1, z_R, μ and m.

Let us now search for such a holo-lens recording and imaging geometry which ensures a good quality of imaging. It is easy to notice that distortion always equals zero (and in consequence, field curvature). It is therefore enough to fix our attention on spherical aberration, coma, and astigmatism.

When analysing the formulae (2), one can see that it is possible to obtain the aplanatic correction. Thus, if we assume that only the primary image is of interest, $m = \mu = 1$ and $z_C = z_R$, then spherical aberration vanishes. It will be assumed then that this condition is always fulfilled in our further analysis. Additionally if $z_1 = -z_R$ then the coma vanishes also, and therefore imaging may be called aplanatic. Such imaging geometry has already been investigated in our earlier paper [3]. However, it appears that the remaining astigmatism is relatively great and the imaging quality is unsatisfactory. It may be worth giving up the aplanatic correction and trying to obtain the imaging of smaller astigmatism even at the expense of the coma reapearance. Such case has been also analysed in our paper [4].

3. Holographic lens of improved imaging quality

Let us now search more precisely for geometrical conditions enabling us to obtain a better quality of imaging of a non-aplanatic holo-lens. For the aberration diminishing it is possible to employ two additional geometrical parameters which have not been taken into account till now. Namely, the holo-lens can be recorded on the curved surface and its input pupil can be shifted before or back of its surface.

3.1. Curved holographic lens

The influence of the hologram bending on the image quality has been investigated by WELFORDT [5], MUSTAFIN [6], and GAJ and KIJEK [7], and most recently VERBOVEN and LAGASSE [8], and WEIGÄRTNER and ROSENBRUCH [9]. On the basis of their results we get – for the holo-lends recorded on spherical surface of the radius ϱ (Fig. 3) – appropriate formulae describing the III-order aberration coefficients (for $m = 1$):

$$
\begin{aligned}
S &= \frac{1}{z_C^3} - \frac{1}{z_3^3} \pm \mu\left(\frac{1}{z_1^3} - \frac{1}{z_R^3}\right) + \frac{2}{\varrho}\left[\frac{1}{z_C^2} - \frac{1}{z_3^2} \pm \mu\left(\frac{1}{z_1^2} - \frac{1}{z_R^2}\right)\right], \\
C &= \frac{x_C}{z_C^3} - \frac{x_3}{z_3^3} + \frac{1}{\varrho}\left(\frac{x_1}{z_1^2} - \frac{x_3}{z_3^2}\right), \qquad (3) \\
A &= \frac{x_C^2}{z_C^2} - \frac{x_3^2}{z_3^2}.
\end{aligned}
$$

Astigmatism does not depend on the holo-lens bending, but it is possible to compensate the coma completely by appropriate choosing of ϱ. The primary image is still free from spherical aberration if $z_C = z_1$.

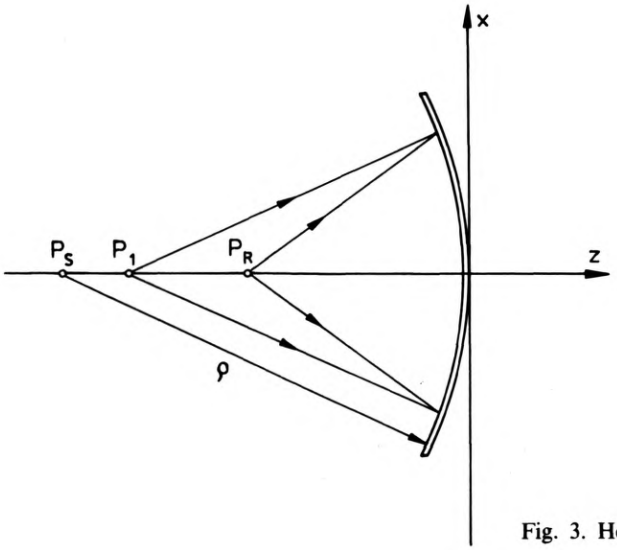

Fig. 3. Holo-lens recorded on the curved surface

3.2. Plane holo-lens with shifted input pupil

The second possibility of the aberration correction is connected with the shifting of the input pupil location off its normal position in the holo-lens plane [8], [11]–[13]. Shifting of this pupil by the value t (Fig. 4) causes a displacement of the holo-lens active area center (effective pupil) by

$$x = x_C \frac{t}{t - z_C}. \tag{4}$$

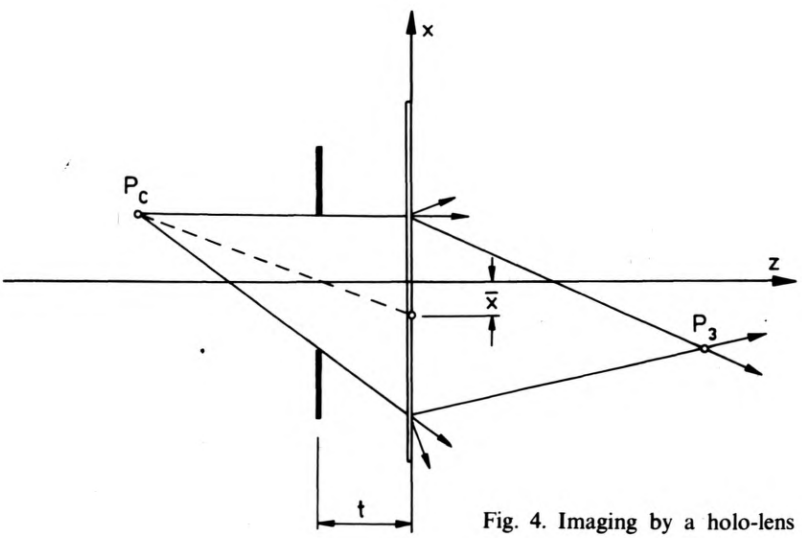

Fig. 4. Imaging by a holo-lens with shifted pupil

The III-order aberration coefficients expressed by the respective aberration coefficients of the "normal" holo-lens and the effective pupil displacement are then:

$$\bar{S} = S,$$
$$\bar{C} = C + \bar{x}S, \tag{5}$$
$$\bar{A} = A - 2\bar{x}C + \bar{x}^2 S.$$

Spherical aberration does not depend on the pupil location, but it may be made equal to zero by identity as has already been stated. Then coma cannot be compensated, but it is possible to eliminate astigmatism.

3.3. Curved holo-lens with shifted input pupil

Unfortunately, it is impossible to compensate completely all aberrations by simultaneous bending of the holo-lens surface and shifting of the input pupil (Fig. 5). However, the image quality can be optimized somewhat by such a choice of

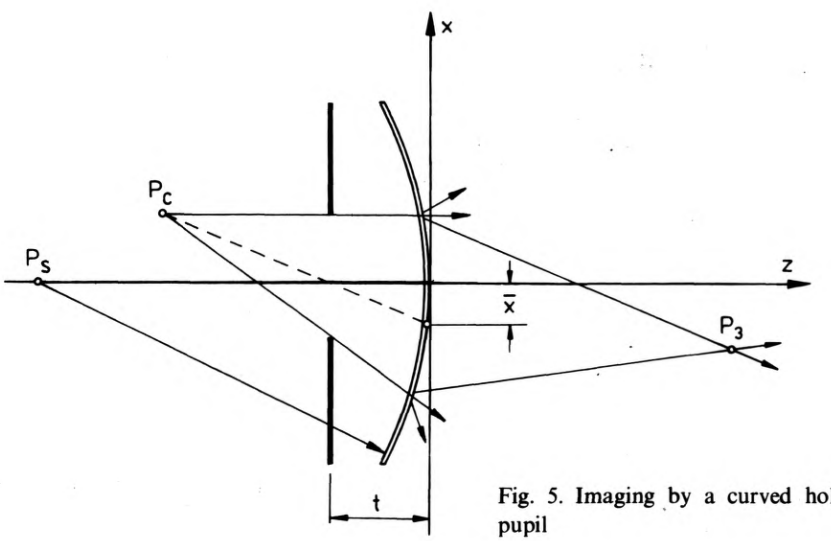

Fig. 5. Imaging by a curved holo-lens with shifted pupil

parameters ϱ and t that for zero spherical aberration, coma and astigmatism would be properly balanced. The admissible values of coma and astigmatism (in consequence, of ϱ and t) should be matched to the definite applications of the holo-lens.

4. Illustrative example

To illustrate the above mentioned possibilities of the imaging quality correction let us analyse the following example. The holo-lens recording geometry is: $z_1 = -100$ mm, $z_R = -150$ mm, $\lambda_1 = 632.8$ nm, lens diameter $\Phi = 10$ mm. The distance from object plane to the lens is: $z_C = z_R = -150$ mm, $\mu = m = 1$. Primary

image (free from spherical aberration) origins in the plane $z_3 = -100$ mm (is a virtual one). The five cases investigated, denoted by the capital letters A–E, are described below.

An image of a point on axis which is obviously aberration-free and serves as a reference is denoted by A. Letter B refers to the image of an off-axis point object for which the object field angle $u = x_C/z_C = 0.04$ given by a flat holo-lens ($\varrho = \infty$) of unshifted pupil ($t = 0$). An image of the same object, but given by the bent lens of the curvature ensuring a full coma compensation and unshifted pupil (unchanged astigmatism) is denoted by C. Letter D relates to the imaging given by the flat holo-lens of the appropriately shifted pupil (unchanged coma and compensated astigmatism) and the same off-axis object. The last case E concerns the "optimum imaging". The appropriately chosen holo-lens curvature as well as pupil shift ensure partial correction of both remaining aberrations.

Those examples have been investigated with the help of the numerical model of imaging by a holo-lens based on the algorithm developed and described in [14] and [15]. The numerical analysis offers a unique possibility of quick and precise image quality evaluation avoiding besides the complicated technological and experimental problems. Quality and quantity of the obtained information appear to be enough for adequate analysis of the influence of particular parameters of the imaging geometry on the image quality.

This algorithm enables us to calculate the complex light amplitude, as well as the light intensity in the image of a point object (in the aberration spot). Having this calculated it is easy to determine the two-point resolution limit for both cases: where the object points are either mutually coherent or incoherent, by evaluation of the light intensity distribution in the appropriate images of two-point object. It is worth noting that for greater aberrations the effect of "false resolution" occurs, so sometimes it is difficult or even impossible to find the resolution limit (comp. [16]).

Since, however, no aberration spot nor two-point resolution characterizes fully the imaging quality it is necessary to perform some additional analysis of the image. Under assumption of isoplanatism it is possible to calculate from the convolution integral the light intensity distribution in the images of any extended objects. In the case of coherent illumination the bar test (Ronchi ruling) of different spatial frequencies seems to be the most interesting. For incoherent illumination the transfer function is usually treated as a good measure of the extended object imaging quality.

All the above mentioned calculations have been conducted one-dimensionally to shorten the computing time; this simplification, however, does not influence essentially the obtained results and presented conclusions.

The results of calculations are shown in the following pictures.

4.1. Aberration spots

Figure 6 presents the aberration spots for the five analysed cases. A characteristic curve of sinc^2 shape is seen in the aberration-free image A. For off-axis imaging (B) the aberrations worsen the image very seriously. Influence of coma is seen in

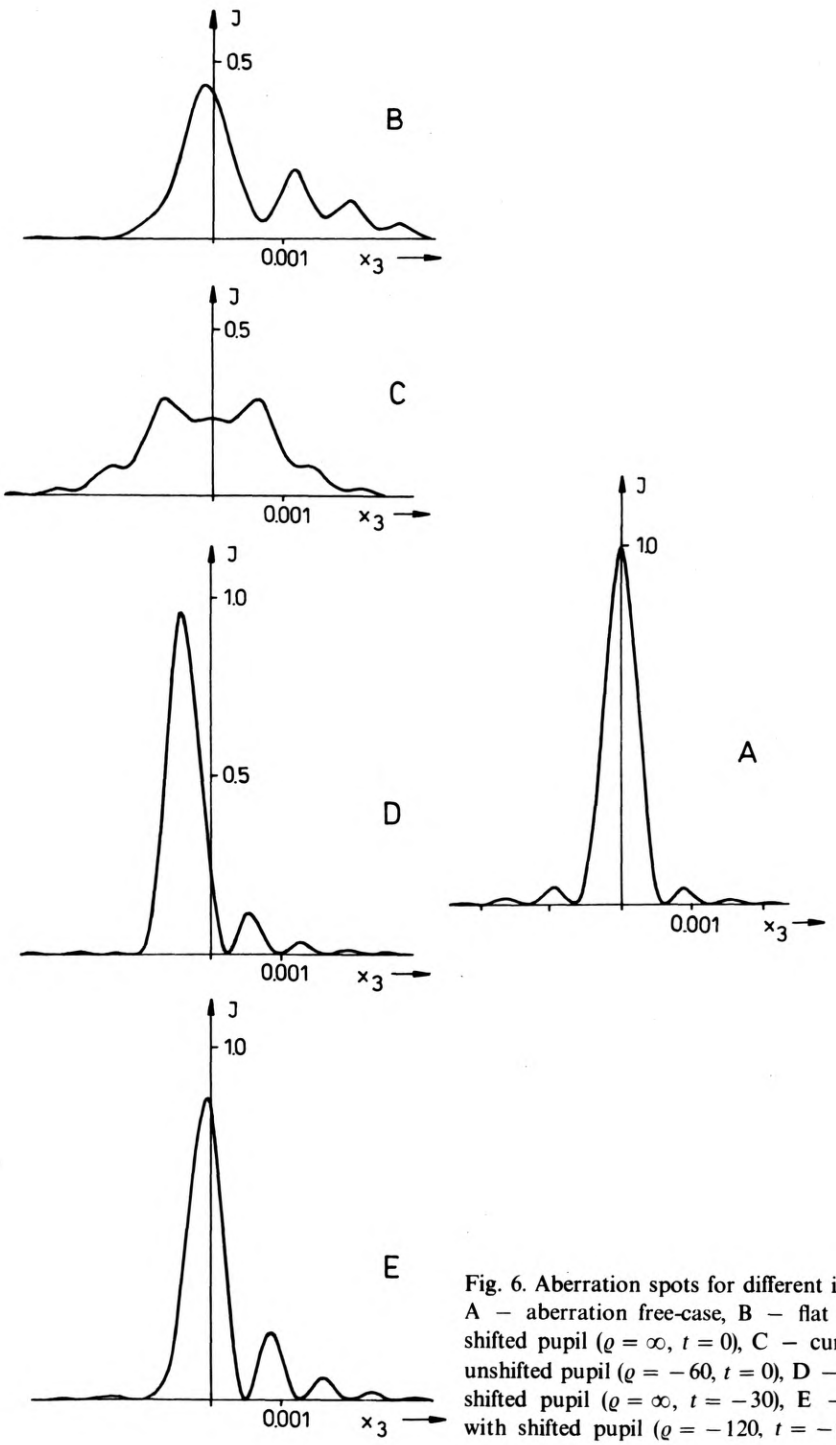

Fig. 6. Aberration spots for different imaging conditions: A – aberration free-case, B – flat holo-lens with unshifted pupil ($\varrho = \infty$, $t = 0$), C – curved holo-lens with unshifted pupil ($\varrho = -60$, $t = 0$), D – flat holo-lens with shifted pupil ($\varrho = \infty$, $t = -30$), E – curved holo-lens with shifted pupil ($\varrho = -120$, $t = -60$)

the spot denoted by D. The holo-lens of the curved surface (C) produces a symmetrical aberration spot (absence of coma) but rather great astigmatism causes that the imaging quality may not be considered satisfactory. Only when both aberrations, coma and astigmatism, are compensated simultaneously (E) the aberration spot seems to be the most similar to the aberration-free one.

The same results are given in the Table. For the five cases (A–E) the following parameters are presented:

– $\bar{x}$, t, ϱ' – describing the lens pupil shifting and its surface bending,

– S, C, A – II-order aberration coefficients.

Quantities characterizing the aberration spot are:

– J_{max} – maximum light intensity, in relation to aberration-free image,

– $d_{0.8}$ – diameter of the spot concering $80^0/_0$ of the encircled energy,

– M_2 – second-order moment of light intensity distribution in the aberration spot which is a measure of its "flatness" defined as

$$M_2 = \int J(x)\, x^2\, dx / \int J(x)\, dx,$$

– M_3 – third-order moment being a measure of aberration spot asymmetry defined as

$$M_3 = \int J(x)\, x^3\, dx / \int J(x)\, dx,$$

and finally

– δ_{coh}, δ_{incoh} – coherent and incoherent two-point resolution limits, respectively.

It can be seen from the Table that the essentially bad image for the field angle 0.04 (case B) is then gradually improved. Compensation of astigmatism (by pupil shifting) follows to the more evident improvement of the image than coma

Some parameters of the holo-lens imaging conditions and image quality measures

		A	B	C	D	E
x_C	[mm]	0	12	12	12	12
t	[mm]	0	0	0	−30	−60
ϱ	[mm]	∞	∞	−60	∞	−120
S	[–]	0	0	0	0	0
$C \times 10^{-6}$	[–]	0	4.44	0	4.44	1.07
$A \times 10^{-6}$	[–]	0	2.13	2.13	0	−0.51
J_{max}	[–]	1.00	0.44	0.23	0.85	0.94
$M_2 \times 10^{-5}$	[mm^2]	2.07	8.97	8.98	3.65	2.44
$M_3 \times 10^{-5}$	[mm^3]	0	5.36	0	3.15	2.07
$d_{0.8}$	[mm]	0.003	0.011	0.012	0.006	0.004
δ_{coh}	[mm]	0.009	0.019*	0.035**	0.011	0.006
δ_{incoh}	[mm]	0.006	0.009	0.020*	0.006	0.006

* "false resolution" occurs,

** value difficult to evaluate.

correction (by surface bending). The last example (E) shows already rather good image correction in which J_{max} does not substantially differ from its aberration-free equivalent. As has already been noted for higher aberration (e.g., examples B, C), the two-point resolution can hardly be used for image quality measurement; however, if all aberrations are reduced (E), the resolution can be easily evaluated and is very much similar to that for the on-axis object.

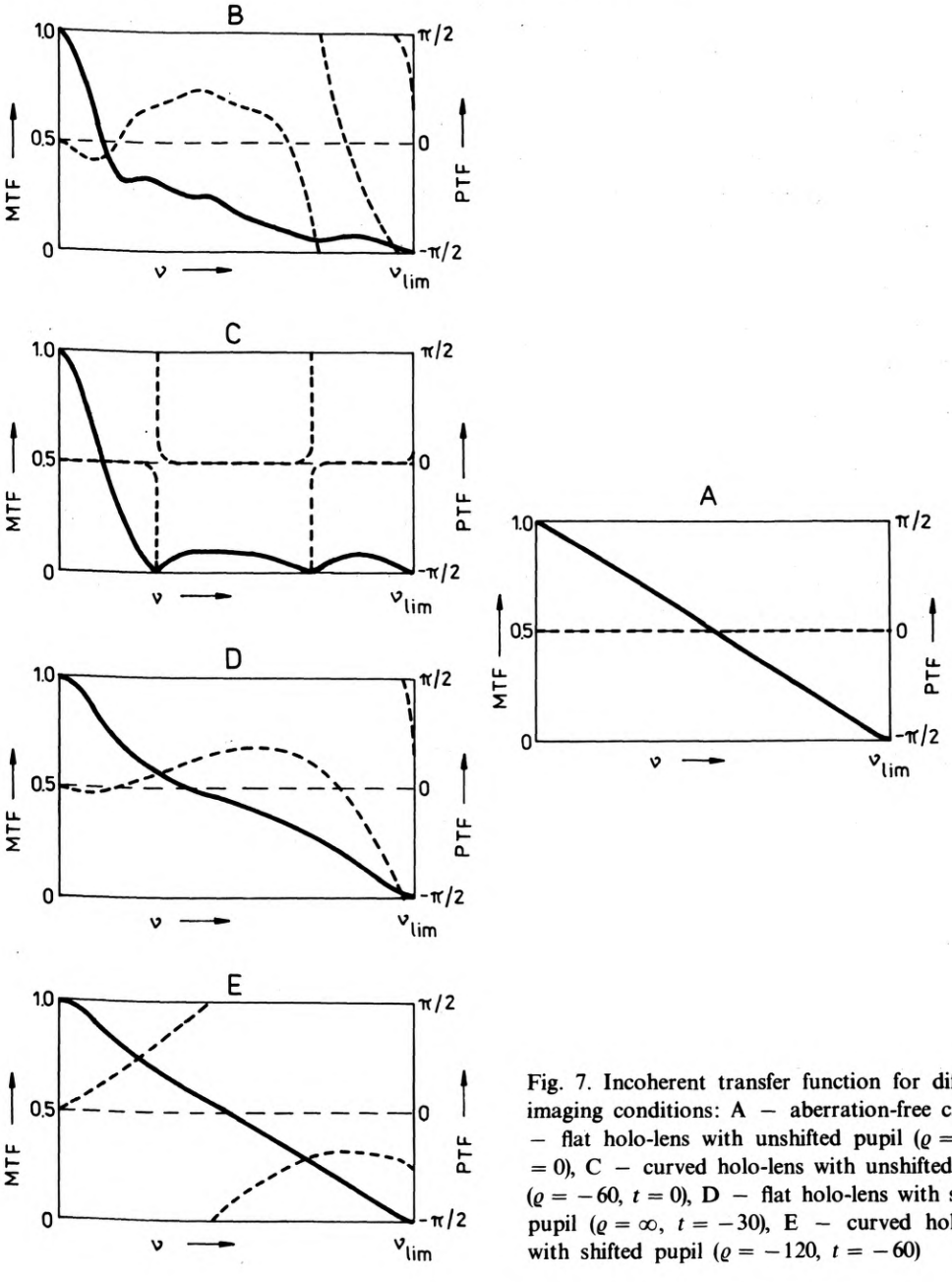

Fig. 7. Incoherent transfer function for different imaging conditions: A – aberration-free case, B – flat holo-lens with unshifted pupil ($\varrho = \infty$, $t = 0$), C – curved holo-lens with unshifted pupil ($\varrho = -60$, $t = 0$), D – flat holo-lens with shifted pupil ($\varrho = \infty$, $t = -30$), E – curved holo-lens with shifted pupil ($\varrho = -120$, $t = -60$)

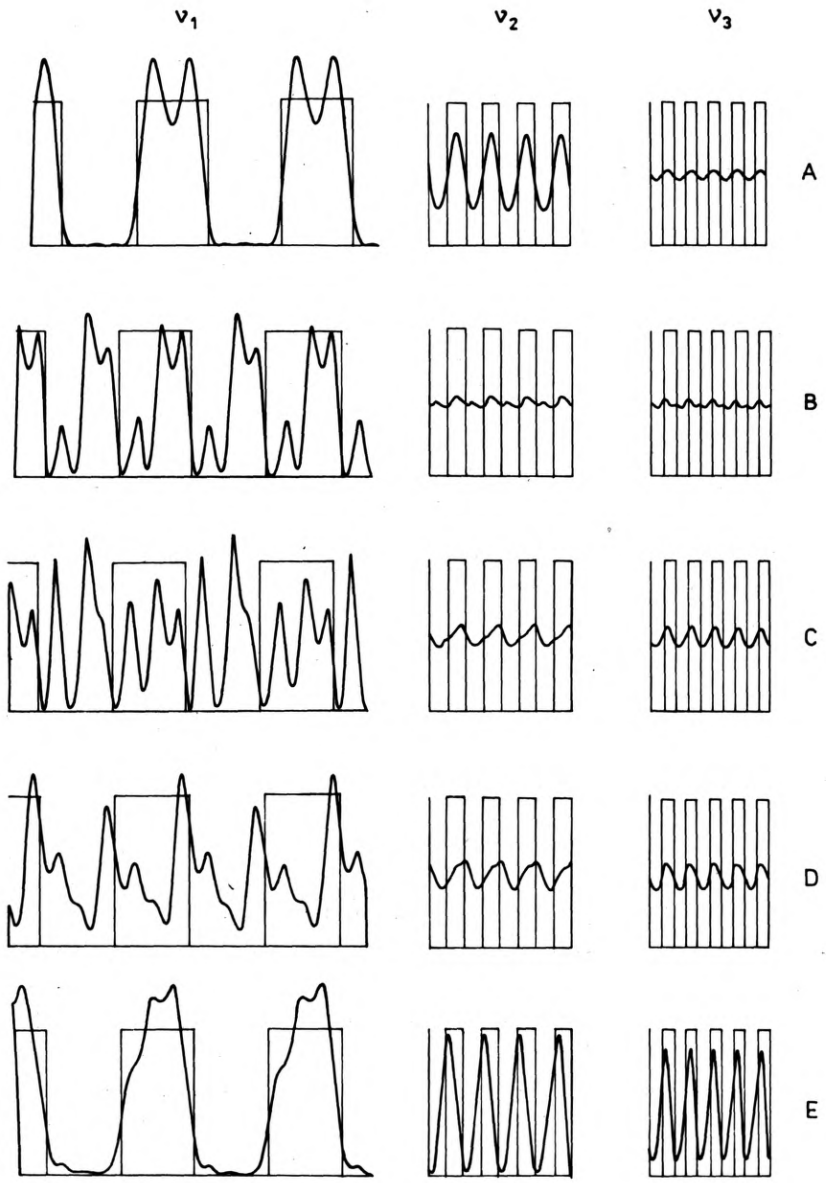

Fig. 8. Coherent images of Ronchi ruling of three spatial frequencies ($\nu_1 = 20$ l/mm, $\nu_2 = 80$ l/mm, $\nu_3 = 120$ l/mm) and different imaging conditions: A – aberration-free case, B – flat holo-lens with unshifted pupil ($\varrho = \infty$, $t = 0$), C – curved holo-lens with unshifted pupil ($\varrho = -60$, $t = 0$), D – flat holo-lens with shifted pupil ($\varrho = \infty$, $t = -30$), E – curved holo-lens with shifted pupil ($\varrho = -120$, $t = -60$)

4.2. Optical transfer function

For estimating the imaging quality of extended objects in incoherent light we have analysed the transfer function. The respective curves illustrating its modulus (MTF) – soild line, and phase (PTF) – dashed line, are shown in Fig. 7. Spatial frequencies v are given in respect to the theoretical cut-off frequency which for the analysed geometry is equal to $v_{\text{lim}} = 165$ l/mm. The conclusions following from the transfer function analysis are similar to those arising from the aberration spot analysis. In the last, best case (E) MTF practically does not differ from its aberration-free equivalent, only the PTF run reflects the influence of coma.

4.3. Images of Ronchi ruling

For the coherent illumination the light intensity distribution in images of Ronchi ruling of three characteristic frequencies $v_1 = 20$ l/mm, $v_2 = 80$ l/mm, $v_3 = 125$ l/mm are presented in Fig. 8. If spatial frequency is low (v_1) the effect of "frequency doubling" may be seen. It is a result of filtering properties of such holo-lens. If the lens is burdened with astigmatism (examples B and C) this effect is so evident that the image is completely deformed. If the spatial frequency is as high as v_3 the image is practically illegible, except for the imaging by a lens of simultaneously compensated coma and astigmatism (E) being even better than for the aberration-free case. The same also follows from the analysis of the coherent resolution limit (comp. Tab.).

5. Conclusions

All the above considerations give evidence to the fact that the holo-lens of appropriately curved surface and shifted pupil can give a good quality image even for relatively large object field angle. On the basis of the presented analysis one can assume that for some applications the single holo-lens may be used for imaging of the extended objects with reasonably large object field angle with satisfactory results if the two parameters, holo-lens surface bending and its input pupil shifting are used for minimizing the aberrations. It seems also that the holo-lens bending has less significant influence on the imaging quality than pupil shifting. It is a comforting fact as from the technological point of view it is much easier to put additional aperture in front of the lens than to record the holo-lens on the curved surface.

References

[1] MEIER R. W., J. Opt. Soc. Am. **55** (1965), 987.
[2] CHAMPAGNE E. B., J. Opt. Soc. Am. **57** (1967), 51.
[3] NOWAK J., ZAJĄC M., Optik **70** (1985), 143.
[4] NOWAK J., ZAJĄC M., [In] *Proc. Image Science '85 Conf.*, Helsinki 1985 [Ed.] A. Friberg, P. O. Oittinen, add. 56.

[5] WELFORDT W. T., J. Phot. Sci. **23** (1975), 84.
[6] MUSTAFIN K. C., Opt. i Spektr. (in Russian) **37** (1974), 1158.
[7] GAJ M., KIJEK A., Opt. Appl. **10** (1980), 341.
[8] VERBOVEN P. E., LAGASSE P. E., Appl. Opt. **25** (1986), 4150.
[9] WEIGARTNER I., ROSENBRUCH M., Optik **73** (1986), 108.
[10] BOBROV S. T. et al., Opt. i Spektr. (in Russian) **46** (1979), 153.
[11] GREYSUKH G. I. et al., Zh. Tekhn. Fiz. (in Russian) **49** (1979), 153.
[12] SMITH R. W., Opt. Commun. **19** (1976), 245.
[13] NOWAK J., ZAJĄC M., Opt. Appl. **11** (1981), 285.
[14] NOWAK J., ZAJĄC M., Opt. Appl. **12** (1982), 253.
[15] NOWAK J., ZAJĄC M., Opt. Acta **30** (1983), 1749.
[16] NOWAK J., ZAJĄC M., Opt. Appl. **14** (1984), 255.

Received May 5, 1987

Нумерические исследования отражения полученного с помощью искривленных голографических линз

Исследовано отражение полученное с помощью голографической линзы, а результаты оценки качества отражения представлены в настоящей работе. Принимали во внимание два случая: когерентного и некогерентного освещения. Принято, что голографическая линза была регистрирована на плоской или сферической поверхности. Проанализовано также влияние положения входного зрачка на качество отражения. Для нескольких типичных параметров геометрии регистрирования линзы и отражения вычислены такие характеристики отражения, как: разложение силы света в аберрационном пятне, двухточечная способность разделения, образы тестов Рончи с избранными пространственными частотами для когерентного освещения и функция переноса контраста для некогерентного освещения.